THE JOURNAL OF PHYSICAL CHEMISTRY B

ARTICLE

pubs.acs.org/JPCB

Role of the HoxZ Subunit in the Electron Transfer Pathway of the Membrane-Bound [NiFe]-Hydrogenase from *Ralstonia eutropha* Immobilized on Electrodes

Murat Sezer,[†] Stefan Frielingsdorf,[‡] Diego Millo,[†] Nina Heidary,[†] Tillman Utesch,[†] Maria-Andrea Mroginski,[†] Bärbel Friedrich,[‡] Peter Hildebrandt,[†] Ingo Zebger,[†] and Inez M. Weidinger[†,*]

[†]Insitut für Chemie, Technische Universität Berlin, Strasse des 17, Juni 135, 10623 Berlin, Germany

[‡]Humboldt-Universität zu Berlin, Chausseestrasse 117, 10115 Berlin, Germany

Supporting Information

ABSTRACT: The role of the diheme cytochrome *b* (HoxZ) subunit in the electron transfer pathway of the membrane-bound [NiFe]-hydrogenase (MBH) heterotrimer from *Ralstonia eutropha* H16 has been investigated. The MBH in its native heterotrimeric state was immobilized on electrodes and subjected to spectroscopic and electrochemical analysis. Surface enhanced resonance Raman spectroscopy was used to monitor the redox and coordination state of the HoxZ heme cofactors while concomitant protein film voltammetric measurements gave insights into the catalytic response of the enzyme on the electrode. The entire MBH heterotrimer as well as its isolated HoxZ subunit were immobilized on silver electrodes coated with self-assembled monolayers of ω-functionalized alkylthiols, displaying the preservation of the native heme pocket structure and an electrical communication between HoxZ and the electrode. For the immobilized MBH heterotrimer, catalytic reduction of the HoxZ heme cofactors was observed upon H_2 addition. The catalytic currents of MBH with and without the HoxZ subunit were measured and compared with the heterogeneous electron transfer rates of the isolated HoxZ. On the basis of the spectroscopic and electrochemical results, we conclude that the HoxZ subunit under these artificial conditions is not primarily involved in the electron transfer to the electrode but plays a crucial role in stabilizing the enzyme on the electrode.

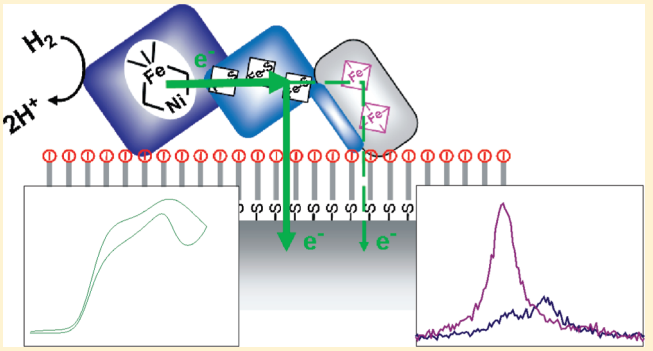

INTRODUCTION

[NiFe]-hydrogenases catalyze the reversible splitting of molecular hydrogen (H_2) into electrons and protons. In view of the growing importance of hydrogen-based technologies in energy storage and conversion, substantial research efforts have been made to explore the potential of these enzymes for biotechnological applications.[1−4] In this respect, oxygen-tolerant hydrogenases, such as the membrane-bound [NiFe]-hydrogenase (MBH) from *Ralstonia eutropha* H16, are of particular interest because they retain considerable catalytic activity even in the presence of atmospheric oxygen concentrations.[1,5,6]

MBH consists of three subunits, HoxG, HoxK, and HoxZ, and thus, the entire purified complex is denoted as HoxGKZ heterotrimer (Figure 1A). The large hydrogenase subunit HoxG contains the catalytic site comprising the bimetallic [NiFe] core that is bound to the protein via four cysteine residues. Furthermore, one CO and two CN^- ligands are coordinated to the Fe. The small subunit HoxK harbors three different iron sulfur clusters acting as an electron relay unit.[7,8] The membrane-integral heme *b*-containing subunit HoxZ anchors the enzyme to the membrane and ensures electron transfer between the hydrogenase dimer HoxGK and the quinone pool of the respiratory chain.[9,10] Although HoxZ is evidently an essential component of the coupling between the catalytic H_2 conversion and the energy transduction machinery, it has been found that the purified, isolated hydrogenase heterodimer, consisting only of the subunits HoxG and HoxK, is catalytically fully active.[11] In fact, most of the previous structural and catalytic studies on MBH were based on the heterodimer HoxGK[1,5−7,12−14] or on intact membrane preparations.[7,15]

In this study, the entire heterotrimeric HoxGKZ complex was isolated and used to analyze the role of HoxZ for the overall catalytic and electron transport processes in more detail. These studies are of particular interest for potential applications of MBH immobilized on electrodes because the optimization of the electronic communication between the catalytic center and the

Received: May 19, 2011
Revised: July 13, 2011
Published: July 15, 2011

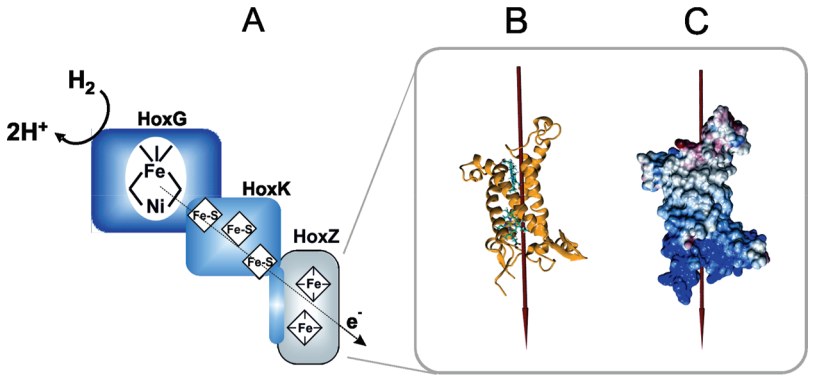

Figure 1. (A) Schematic representation of the whole MBH heterotrimer HoxGKZ, (B) homology model, and (C) calculated surface potential distribution of the modeled HoxZ subunit. Positively charged groups are depicted in blue, and negatively charged groups are depicted in red. The arrows in parts B and C indicate the direction of the calculated dipole moment.

conducting support material is one of the crucial challenges for exploiting hydrogenases as a catalyst.

To elucidate the role of the HoxZ subunit in heterogeneous electron transfer between the immobilized enzyme and the electrode during the catalytic process, biocompatibly coated electrodes were employed that allow the immobilization of enzyme preparations under the preservation of the native structure and function, as shown in previous studies of other redox enzymes.[16−18] To probe electric communication between enzymes and electrodes, electrochemical methods such as protein film voltammetry (PFV) are usually employed. This technique, however, monitors only the current flow from the enzyme to the electrode and vice versa, whereas structural information on the redox cofactors cannot be obtained. This disadvantage can be overcome by employing surface sensitive vibrational spectroscopy such as surface enhanced infrared absorption (SEIRA) spectroscopy, which has been successfully used to probe CN^- and CO ligands of the catalytic center under turnover and nonturnover conditions of immobilized hydrogenases.[19−21] To monitor the two heme *b* cofactors of HoxZ, which is in the focus of the present study, surface enhanced resonance Raman (SERR) spectroscopy is the method of choice. This technique combines the surface enhanced Raman effect, that is, the amplification of the radiation field due to the coupling with the surface plasmons of the metallic support, with the molecular resonance Raman (RR) effect. For heme cofactors, optimum resonance conditions for both the plasmonic and the molecular electronic transitions are achieved by using excitation lines in the violet spectral region and nanostructured silver support materials. Under these conditions, the SERR spectra exclusively display the vibrational bands of the cofactors solely of the immobilized heme proteins. Thus, it is possible to selectively monitor the redox and conformational states of the cofactors of the immobilized HoxZ subunit during the catalytic cycle and to analyze the dynamics of heterogeneous electron transfer between the heme cofactors and the electrode. In combination with electrochemical and theoretical methods, the spectroscopic data provide novel insight into the involvement of the HoxZ subunit in the catalytic processes of immobilized MBH.

MATERIALS AND METHODS

Chemicals. 6-Amino-1-hexanethiol hydrochloride [C6(NH_2)] and 5-carboxyl-1-pentanethiol [C5(COOH)] were purchased from Dojindo; 6-mercaptohexanol [C6(OH)] and digitonin were purchased from Serva; *n*-dodecyl-β-D-maltoside (β-DDM) (crystallography grade) and 7-mercaptoheptane were purchased from Applichem and Fluka, respectively. All chemicals were of highest purity grade available.

Protein Purification. In brief, the MBH heterotrimer HoxGKZ was purified after solubilization with digitonin via a C-terminal *Strep-tag* II at the HoxZ subunit. Isolation of the HoxZ subunit was performed in a similar way but using β-DDM as a detergent instead of digitonin. The detailed purification protocol of the proteins used in this study will be published elsewhere.[22]

Protein Immobilization. Electrochemically roughened Ag electrodes were immersed for 24 h in solutions of ω-substituted mercaptanes to form a self-assembled monolayer (SAM). For pure SAMs, 1 mM of C6(NH_2) or C5(COOH) was dissolved in a water/ethanol mixture (1:4 v/v) or pure ethanol. For mixed SAMs, 1 mM C6(NH_2) or C5(COOH) was mixed with 3 mM C6(OH) in a water/ethanol solution (1:4 v/v) or in pure ethanol, respectively. Immobilization of the isolated HoxZ subunit, the heterodimer HoxGK, and the entire MBH heterotrimer HoxGKZ was achieved by the immersion (3−5 h) of SAM coated Ag electrodes into a 10 mM potassium phosphate buffer (PB) solution containing ca. 0.4 μM of the respective protein as well as β-DDM in the case of HoxZ and digitonin in the case of HoxGKZ/HoxGK.

Spectroscopic and Electrochemical Measurements. A rotating cuvette was used for RR experiments. The protein concentration was ca.15 μM in 50 mM PB buffer solution at pH 7.0 containing 150 mM NaCl and 0.01% w/w β-DDM.

The SERR and electrochemical measurements were performed using homemade spectroelectrochemical cells with a volume of about 10 mL, a rotating Ag ring with a geometrical area of 0.75 ± 0.05 cm^2 as the working electrode, an Ag/AgCl (3 M KCl) reference electrode (+0.21 V vs SHE), and a platinum counter electrode. All potentials cited in this work refer to the standard hydrogen electrode (SHE). The buffer solutions used for the SERR spectroscopic and electrochemical experiments were adjusted to the same pH as the respective incubation buffers but did not contain any detergent.

SERR and RR spectra were measured using a confocal Raman spectrometer (LabRam HR 800, Jobin Yvon) coupled to a liquid nitrogen cooled CCD detector. The spectral resolution was 1 cm^{-1} with an increment per data point of 0.75 cm^{-1}. The 413 nm laser line of a Coherent Innova 400 Krypton cw-laser was used for excitation. The laser power on the sample was 2.0 mW for RR and 1.0 mW for SERR experiments. The laser beam was

focused onto the sample by a Nikon 20× objective with a working distance of 20.5 mm and a numeric aperture of 0.35.

The accumulation times of the SERR spectra were between 1 and 10 s, whereas, for the RR spectra, the accumulation time was 30 s. Time-resolved (TR) SERR experiments were carried out as described previously.[23] After the polynomial baseline subtraction, the measured spectra were treated with homemade component analysis software.

UV/vis spectroelectrochemical redox titrations of the isolated HoxZ subunit in solution were performed using a transmission cell that has been described elsewhere.[24] UV−vis absorption spectra were recorded using a Cary 50 spectrometer, while the cell potential was controlled with a EG&G 263A potentiostat. The solution used for the spectroelectrochemical measurements included 100 mM PB, 150 mM NaCl, and 0.01% w/w β-DDM but no additional redox mediators.

Cyclic voltammetric experiments were performed with a CH instrument 660 C (Austin, TX, U.S.A.).

Molecular Modeling and Theoretical Calculations. Modeling was performed with the Swiss model server[25] using the fdnI subunit of the formate dehydrogenase-N (pdb accession code 1kqg) as a template structure.[26] The modeled residue range was 26−243, the sequence identity between the model and the template is 9.174%, and the e-value was 1.0×10^{-38}. Dipole moment calculations were carried out with VMD 1.8.7[27] with the partial charges of the CHARMM22 force field.[28] For the determination of the electrostatic potential, we have utilized the APBS program[29] and the PDB2PQR tool.[30]

RESULTS

Calculation of the HoxZ Surface Potential Distribution. Because of the lack of structural information on the HoxZ subunit, a homology model was generated to calculate the electrostatic potential and the dipole moment of this protein (Figure 1B). The fdnI subunit of the formate dehydrogenase-N from *E. coli* served as template. A previous study reported on the basis of sequence analyses shows that these two proteins are structurally related,[31] such that the model is expected to represent a good approximation for HoxZ. HoxZ contains two *b*-type hemes, each of them carrying two axial His ligands. The distance between the heme irons in the model is 19.2 Å while the distance between the edges of the porphyrin π-electron system is 7.5 Å, enabling direct electron tunneling between the two heme groups.[32] According to this structural model and surface potential calculations, HoxZ possesses a cylindrical shape with a slightly negatively charged upper and a positively charged bottom side. The latter accommodates the C- and N-terminal regions and a mainly hydrophobic lateral area forming contacts with the bilayer core of the membrane (Figure 1C). The dipole moment was calculated to be ca. 1100 D in the fully reduced state (Fe^{2+}/Fe^{2+}).

SERR Spectroscopic Investigation of the HoxZ Subunit. The RR spectra of the isolated HoxZ subunit show the vibrational signature characteristic of six-coordinated low-spin (6cLS) hemes as expected for bis-His ligated coordination (Figure 2A and E). The symmetric band shapes point to essentially identical RR spectra for both heme groups. Upon the immobilization of HoxZ on SAM coated Ag electrodes, strong SERR-signals were detected when using C6(NH_2) or C5(COOH) SAMs at pH 7.0 and low ionic strength (10 mM PB). However, the SERR spectra differ from the RR spectrum, inter alia, by a broadening of the ν_4 envelope and an additional peak ν_3 band region at 1491 cm^{-1},

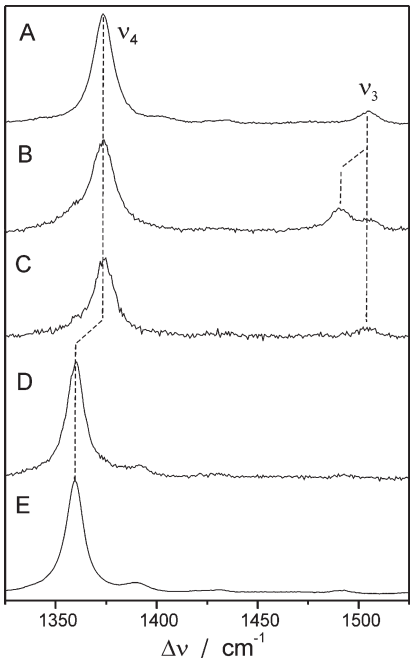

Figure 2. (A) RR spectrum of the isolated, fully oxidized HoxZ subunit in solution. (B) SERR spectrum of the isolated HoxZ subunit immobilized on a C5(COOH) SAM at the electrode potential E = +0.3 V. (C) SERR spectra of the whole HoxGKZ heterotrimer immobilized on a C5(COOH) SAM at E = +0.3 V. (D) SERR spectra of the whole HoxGKZ heterotrimer immobilized on a C5(COOH) SAM at E = −0.27 V. (E) RR spectrum of the fully reduced HoxZ subunit. Further experimental conditions: (A, E) 50 mM PB at pH 7.0, 0.15 M KCl, and 0.01% β-DDM; (B) 10 mM PB at pH 7.0; (C, D) 0.1 M PB at pH 5.5.

which is characteristic of five-coordinated high-spin (5cHS) heme (Figure 2B). This conclusion is confirmed by the component analysis of the spectra that allows quantifying the relative contributions of the various species involved.[33]

The relative contribution of the 5cHS species is higher for C5(COOH) SAMs than it is for C6(NH_2) SAMs, but it decreases in both cases in favor of the 6cLS species upon increasing the ionic strength and by an admixture of C6(OH) at a ratio of 3:1 [C6(OH)/C5(COOH) and C6(OH)/C6(NH_2)] (Table S1 in the Supporting Information). Both effects are accompanied by a loss of absolute intensity that reflects a partial HoxZ subunit desorption due to weakening of the electrostatic interactions between the subunit and the SAM. In the case of the carboxyl-terminated SAM, the 5cHS content was further diminished by decreasing the pH from 7.0 to 5.5. However, a similar decrease in pH in the case of C6(NH_2) SAMs led to a complete loss in signal intensity.

The structural perturbations were largely avoided upon using C5(COOH) SAMs at pH 5.5 and an ionic strength of 100 mM. These conditions represent an acceptable compromise between the preservation of the structural integrity of the immobilized HoxZ and the amount of the adsorbed protein, and thus, they were adopted for the SERR spectroscopic studies of the whole heterotrimer HoxGKZ.

Figure 2C displays the SERR spectrum of the oxidized HoxGKZ at an electrode potential of E = 0.3 V. Note that the total SERR intensity is weaker by a factor of ca. 15 as compared to the case of the isolated HoxZ subunit under the same conditions. This is attributed to the lower surface coverage due

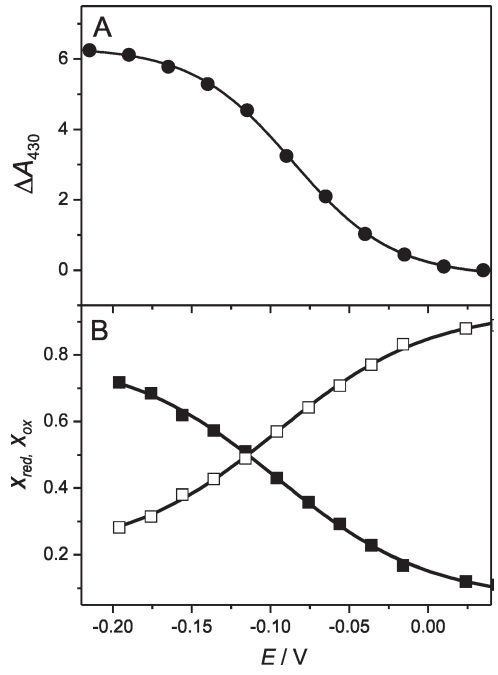

Figure 3. (A) Relative changes in the absorbance at 430 nm of the isolated HoxZ subunit in solution as a function of electrode potential. The reference spectrum was taken at +0.3 V. (B) Potentiometric titration of the HoxZ domain within the MBH heterotrimer immobilized on C5(COOH) coated electrodes at pH 5.5 (0.1 M PBS): x_{red} (solid squares); x_{ox} (open squares).

to the significantly larger size of the whole enzyme.[34] Upon lowering the electrode potential to −0.27 V, the heme cofactors were reduced (Figure 2D). The spectra of the ferrous and ferric forms of the heme included no contributions from a HS species. Furthermore, it should be noted that the cofactors of the HoxG and HoxK subunits do not contribute to the SERR spectrum of the heterotrimer.

Redox Transitions. UV/vis spectroelectrochemical redox titrations of the isolated HoxZ subunit in solution were performed by monitoring the intensity of the Soret band at 430 nm, corresponding to the maximum absorbance of the ferrous heme *b* (Figure 3A). Upon variation of the applied potential, one sharp redox transition having a midpoint potential ($E_{m,sol}$) at −0.086 V was detected. The transition showed an almost ideal Nernstian behavior yielding an apparent number of transferred electrons close to 1 (n = 0.8). The redox transition of the immobilized HoxZ subunit, either isolated or as a constituent of the MBH heterotrimer, was probed by potential-dependent SERR spectroscopy. The relative spectral contributions derived from the component analysis of the spectra were converted into relative concentrations using the proportionality factors determined from the RR spectra of the isolated HoxZ subunit in solution. The corresponding factor for the 5cHS species was taken from a previous study of cytochrome *c*.[33]

Figure 3B shows the molar fractions of the ferric and ferrous state of the HoxZ subunit within the HoxGKZ trimer as a function of applied potential, determined under conditions that suppressed the formation of the 5cHS species (100 mM PBS, pH 5.5, C5(COOH) SAM). The data show a clear redox transition with a midpoint potential at E_m = −0.09 V similar to the $E_{m,sol}$ of the isolated HoxZ subunit in solution but within a significantly broader potential window expressed by a smaller apparent number of transferred electrons (n = 0.5, Table 1). This low value for n may reflect a broadened distribution for the midpoint potentials of the two hemes. Alternatively, it is also consistent with the superposition of the redox transitions for two spectroscopically indistinguishable hemes exhibiting slightly different but discrete E_m values.

Table 1. Redox Properties of the Immobilized HoxZ Subunit in Its Isolated Form and Integrated in the HoxGKZ Heterotrimer[a]

protein	isolated HoxZ subunit	HoxZ in the hetrotrimer
SAM	C5(COOH)/C6(OH) (1:3)	C5(COOH)
E_m/V	−0.085 ± 0.02	−0.09 ± 0.01
n	0.49 ± 0.07	0.52 ± 0.02
k/s^{-1}	0.24 ± 0.06	0.24 ± 0.06

[a] The data refer to the 6cLS species (100 mM PB, pH 5.5).

The redox transition was completely reversible, with the majority of the immobilized proteins remaining electroactive at the surface; however, a complete reduction was not possible as a result of the lower limit of the accessible potential range for SAM coated electrodes[20] (i.e., ca. −0.3 V). The redox titration of the isolated HoxZ subunit displays essentially the same potentiometric behavior (Figure S1C in the Supporting Information). This suggests that the HoxZ subunit is, in both cases, adsorbed similarly.

Under conditions where the 5cHS and 6cLS species coexist, redox titrations of the isolated HoxZ subunit exhibit a similar redox behavior for both species throughout the entire potential range that has been investigated (Figure S1A and B in the Supporting Information). The midpoint potential of the HS species is E_m(HS) = −0.1 V, and thus, it is slightly more positive than E_m(LS) = −0.14 V (see Table S1 in the Supporting Information). One should note that the difference in E_m between the 5cHS and 6cLS species is the same as that observed for the bis-His coordinated B2 state of cytochrome *c*.[33]

In all redox titrations of the isolated HoxZ, a distinct midpoint potential E_m is observed below −0.08 V. E_m is found to increase from −0.15 V (C5(COOH), pH 7.0, 10 mM PB) to more positive values with increasing ionic strength and decreasing charge density on the SAM surface (Table S1 in the Supporting Information) until, at mixed C5(COOH)/C6(OH) SAMs and pH 5.5 (100 mM PB), it approaches the value determined for the HoxZ subunit in solution ($E_{m,sol}$ = −0.086 V). No difference was noted for E_m and n values when comparing the isolated and MBH-integrated HoxZ subunit (Table 1).

TR SERR spectroscopic experiments were carried out to determine the formal heterogeneous electron transfer rate constant (k, hereby obtained at ΔG = 0 eV). For both the isolated HoxZ subunits and MBH complex integral HoxZ subunits, the same value of 0.24 ± 0.06 s^{-1} was determined.

Electron Transfer and Catalytic Activity of the Immobilized Heterotrimer. The participation of the HoxZ subunit in the H_2-dependent electron transfer process of the immobilized heterotrimer was investigated by SERR spectroscopy. The inset in Figure 4 shows the SERR spectra of the HoxZ subunit within the heterotrimer immobilized on the electrode at open circuit. The heme *b* cofactors are almost fully oxidized under Ar atmosphere, as revealed by the prominent band at 1374 cm^{-1}. Purging the solution with H_2, however, leads to a fast reduction of the

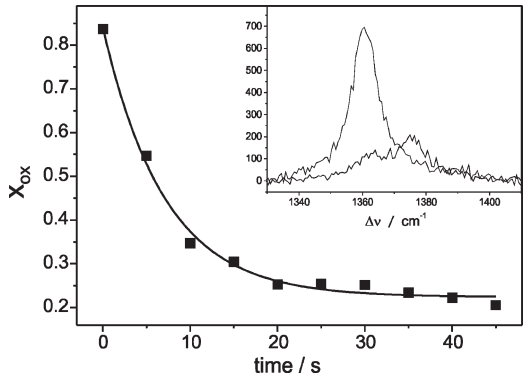

Figure 4. Relative concentration of the oxidized LS species of the entire heterotrimeric enzyme immobilized on C5(COOH) SAMs measured at open circuit in a solution of 100 mM PB at pH 5.5, as a function of time after purging with H_2. Inset: SERR spectra before (black) and 10 s after (gray) purging with H_2.

hemes. Similar experiments performed with the isolated HoxZ subunit did not cause any heme reduction upon purging with H_2 (data not shown). This finding indicates that also—in analogy to the electron transfer pathway under physiological conditions—in the immobilized state, the electronic communication between the catalytic center and the HoxZ subunit is largely preserved.

SERR spectra measured consecutively following H_2 injection allowed the determination of the rate of H_2 induced heme *b* reduction (Figure 4), yielding a value of $0.15 \pm 0.05\ s^{-1}$. Note that this value represents an apparent rate constant of the overall reduction process that may be limited either by the reductive activation of the active site in the HoxG subunit or by the electronic communication between the HoxGK heterodimer and the HoxZ subunit. Also, partial limitation due to incomplete H_2 saturation in solution at the beginning of the experiment cannot be ruled out. Therefore, the measured rate can be seen as a minimum value for intramolecular electron transfer between HoxGK and HoxZ.

However, this rate is at least 60 times higher than the respective value obtained from a similar experiment with the [NiFe] hydrogenase from *Desulfovibrio vulgaris* Miyazaki F.[20,35] It was also shown before that the activation of "standard" (i.e., oxygen-sensitive) hydrogenases is much slower in comparison to the case of oxygen-tolerant hydrogenases.[6] The present data, therefore, clearly indicate an intact electrical communication between the subunits characteristic of the immobilized oxygen-tolerant MBH.

After demonstrating the electrical communication of the HoxZ subunit, with the HoxGK heterodimer on one hand and the electrode on the other hand, the overall electrochemical response of the immobilized HoxGKZ heterotrimer was studied with PFV. The voltammetric signal recorded on a stationary electrode in solutions free of H_2 (Ar atmosphere) is shown in Figure 5A. The negative current at −0.3 V corresponds to proton reduction. The H_2 produced by the enzyme, at negative applied potentials, remains close to the electrode surface and is consumed in the reverse scan direction, exhibiting the sharp catalytic oxidative peak at −0.24 V, similar to that of the standard [NiFe]-hydrogenase from *Allochromatium vinosum* adsorbed at stationary carbon electrodes.[36] The broad peak at −0.12 V is ascribed to the non-Faradic current of the protonation−deprotonation equilibria of the SAM.[37]

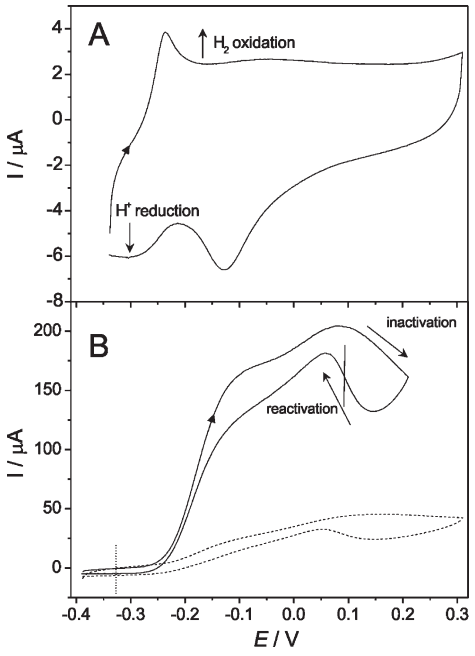

Figure 5. (A) Proton reduction and H_2 reoxidation by the heterotrimer adsorbed on a stationary electrode under Ar gas atmosphere. Scan direction is indicated by arrowheads. (B) Anaerobic inactivation and reductive reactivation (arrows) of the heterotrimer (solid line) and heterodimer (dashed line) immobilized on a C5(COOH) SAM under H_2 gas atmosphere. Scan direction is indicated by an arrowhead; E_{switch} is marked by a vertical bar. The dotted vertical line indicates the potential of the H^+/H_2 couple under the experimental conditions (1 bar H_2, pH 5.5). The electrode was rotated at 400 rpm. Voltammograms were recorded at room temperature in solutions of 100 mM PB at a scan rate of $\nu = 5\ mV\ s^{-1}$. Other conditions are the same as for part A.

Figure 5B shows the voltammetric trace of the immobilized HoxGKZ heterotrimer under H_2 gas atmosphere. The sigmoidal-shaped plot is ascribed to enzymatic H_2 oxidation. This process has an onset potential of −0.26 V, which is more positive by 0.07 V than the potential of the H^+/H_2 couple (Figure 5B, vertical dotted line). Contrary to measurements under Ar atmosphere, H^+ reduction was not observed for the heterotrimer under H_2 atmosphere, probably because of product inhibition of this enzyme (i.e., at 1 bar H_2, proton reduction is suppressed[34]). The arrows indicate the anaerobic inactivation and the reductive reactivation of the enzyme. The corresponding switch potential (E_{switch}), denoted as the potential of maximum slope in the reductive reactivation direction,[34] is equal to 0.09 V. This value, which is related to the reactivation process,[38] is comparable to that obtained for the heterodimer on a pyrolytic graphite electrode (PGE) under similar experimental conditions, revealing comparable inflections at similar potentials.[39]

On the time scale of the experiments, the intensity of the catalytic current diminishes, although the overall shape of the voltammetric signal remains unchanged, thus indicating a reversible redox behavior. The loss of current, quantified by comparing the loss between two consecutive scans, is about 5−10% (Figure S2 in the Supporting Information). This behavior, already reported for the standard [NiFe]-hydrogenase from *Desulfovibrio vulgaris* Miyazaki F, is ascribed to either the irreversible degradation of the active site, caused by reactive oxygen species generated at the electrode during the voltammetric experiment,[20] or enzyme desorption.[34]

To further elucidate the role of the HoxZ subunit in the catalytic electron transfer pathway, voltammetric experiments were also performed on the HoxGK heterodimer immobilized under the same experimental conditions as applied for the HoxGKZ heterotrimer. Although, in this case, the HoxZ subunit was absent, a protein film was formed, affording the same voltammetric shape as the HoxGKZ heterotrimer albeit with a much lower current (Figure 5B).

DISCUSSION

Immobilization. Surface potential calculations for the homology model of HoxZ reveal a positively charged binding domain that is likely to interact with the negatively charged or polar headgroups of the SAM. This conclusion is consistent with the observation that the extent of adsorption, as reflected by the SERR intensity, decreases with lowering the charge density on carboxyl-terminated SAMs and thus weakening the electrostatic interactions with the protein either by decreasing the pH, increasing the ionic strength, or diluting the portion of carboxyl head groups via admixture of hydroxyl-terminated mercaptanes. Electrostatic interactions control not only the adsorption equilibrium but also the structure of the cofactor sites of the immobilized protein. Analogously to previous findings for other heme proteins, strong local electrostatic fields are evidently capable of causing the dissociation of an axial ligand from the heme.[16,33,40] Thus, we conclude that the 5cHS species observed for the immobilized isolated HoxZ under strong electrostatic binding interactions refers to the heme *b* that is in closest proximity to the SAM surface.

A C5(COOH) SAM in 100 mM PB at pH 5.5 is associated by electrostatic interactions with the isolated HoxZ subunit and the MBH complex-integral HoxZ subunit that are too weak to perturb the structure of the heme in closest proximity to the SAM but are strong enough to allow the binding of the protein to an extent that is sufficient for the spectroscopic and electrochemical characterization. Finally, the strength of the electrostatic interaction is also reflected by the redox potential shift ΔE_{RC} defined as the difference between the redox potential of the immobilized protein ($E_{m,SAM}$) and the protein in solution ($E_{m,sol}$). ΔE_{RC} generally decreases with decreasing strengths of electrostatic interactions,[41] which is consistent with the observed trend for ΔE_{RC} in this work.

It is interesting to note that two separated redox potentials at +0.01 V and +0.16 V were reported for the HoxZ subunit of MBH in membrane fragments[9] whereas spectroelectrochemical titrations of the isolated HoxZ subunit and MBH complex-integral HoxZ subunit carried out in this work display only one redox transition around −0.09 V.

Attempts to immobilize HoxZ via the weakly negatively charged top side did not lead to unambiguous conclusions. Immobilizing the isolated HoxZ subunit on C6(NH_2) SAMs in neutral solutions afforded essentially the same redox potential as that determined for C5(COOH) SAMs. Under these conditions, HoxZ might be immobilized via the cationic bottom side, possibly via hydrogen bonding interactions to the nonprotonated amino groups of the SAM. This conclusion is supported by the fact that decreasing the pH, corresponding to an increasing degree of protonation of the SAM, causes a decrease of the amount of adsorbed proteins such that, at pH 5.5, no SERR spectrum can be obtained.

Electrical Communication and Catalytic Activity of the Immobilized HoxGKZ Heterotrimer. It was shown that the immobilized heterotrimer is able to catalytically oxidize hydrogen and deliver electrons from its active site in HoxG to the HoxZ subunit. However, it is very unlikely that the HoxZ subunit is primarily involved in the transfer of these electrons to the electrode as observed in PFV experiments. On one hand, the onset potential of the catalytic current is around −0.26 V, which is far below the redox potential of the HoxZ. Therefore, both hemes of the subunit should be reduced at this electrode potential and, hence, not be able to accept electrons. On the other hand, the heterogeneous electron transfer rate determined by TR SERR spectroscopy ($k = 0.24 \pm 0.06\ s^{-1}$) is too small to account for the strong catalytic current observed in PFV experiments, considering a turnover number of $k_{cat} = 250\ s^{-1}$ estimated for the heterodimer on PGE.[6] The poor electron transfer from HoxZ to the electrode might be due to sterical hindrances caused by the detergent surrounding hydrophobic patches of HoxZ. On the basis of these considerations, the voltammetric signal shown in Figure 5B is not mainly attributable to a heterotrimer shuttling electrons through the HoxZ subunit. At first sight, the CV signal might be attributed to a fraction of heterodimer dissociated from the heterotrimer upon immobilization. This assumption, however, can be excluded because a voltammetric film consisting of the heterodimer only revealed a lower catalytic current. Although this finding shows that the heterodimer alone may bind to the electrode upon retention of catalytic activity, further stabilization of the enzyme on the electrode is achieved by the HoxZ subunit.

It has to be noted at this point that, in its biological context, the HoxZ subunit unambiguously fulfills two functions: (i) anchoring the hydrogenase module to the membrane, and (ii) transferring electrons to the quinone pool.[9,42] On the electrode, HoxZ mainly performs a stabilizing function that could be related to its anchoring function in biological systems. Also, an additional stabilizing function as an electron sink or supply should be considered.

Accordingly, we propose that immobilization preserves essentially the heterotrimer structure but opens two different electron pathways for electronic communication with the electrode: a slow one, transferring electrons from the distal Fe−S cluster to HoxZ and finally to the electrode, and a fast one, transferring electrons directly from the distal FeS cluster to the electrode. Whereas the slow HoxZ-mediated electron transfer is exclusively probed by SERR spectroscopy by monitoring the heme reduction, PFV mainly probes the bypass from HoxK to the electrode. These two electron pathways are drawn schematically in Figure 6.

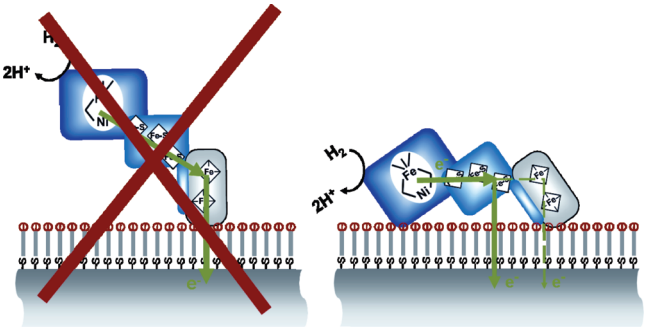

Figure 6. Schematic representation of the proposed electron transfer pathways for the HoxGKZ heterotrimer on electrodes.

CONCLUSIONS

Combined electrochemistry and SERR techniques were used to characterize the membrane-bound [NiFe]-hydrogenase heterotrimer HoxGKZ and its isolated HoxZ subunit. Comparing the behavior of the whole enzyme with that of the HoxZ subunit, a model was derived to rationalize enzyme/electrode interactions. This model suggests that the heterotrimeric unit is immobilized on the SAM coated electrode via the positively charged side of the HoxZ subunit. The native heme pocket structure and the electrical communication between the HoxZ and the HoxGK subunits are largely preserved upon immobilization. However, as a result of a presumably close vicinity of the distal Fe−S cluster of the HoxGK heterodimeric module to the electrode, the electrons may be transferred from the active site of the enzyme to the electrode via two independent pathways: a route associated with a slow overall rate proceeding via the HoxZ subunit and a faster pathway via the HoxGK module. In this scenario, the role played by the HoxZ subunit is not crucial for the electron transfer process, but it contributes to the stabilization of the enzyme on the electrode.

ASSOCIATED CONTENT

Supporting Information. Additional data on the different immobilization strategies and the potentiometric titration of the isolated HoxZ subunit. This material is available free of charge via the Internet at http://pubs.acs.org.

AUTHOR INFORMATION

Corresponding Author

*E-mail: i.weidinger@mailbox.tu-berlin.de. Phone +493031422780. Fax: +493031421122.

ACKNOWLEDGMENT

The authors would like to thank the DFG (Cluster of Excellence, UniCat), the Fonds der Chemischen Industrie (I.W.), and the Alexander von Humboldt Foundation (D.M.).

REFERENCES

(1) Vincent, K. A.; Cracknell, J. A.; Lenz, O.; Zebger, I.; Friedrich, B.; Armstrong, F. A. *Proc. Natl. Acad. Sci. U.S.A.* **2005**, *102*, 16951–16954.

(2) Cammack, R.; Frey, M.; Robson, R. *Hydrogen as a Fuel: Learning From Nature*; Taylor & Francis: London, 2001.

(3) Krassen, H.; Schwarze, A.; Friedrich, B.; Ataka, K.; Lenz, O.; Heberle, J. *ACS Nano* **2009**, *3*, 4055–4061.

(4) Friedrich, B.; Fritsch, J.; Lenz, O. *Curr. Opin. Biotechnol.* **2011**, *22*, 358–364.

(5) Ludwig, M.; Cracknell, J. A.; Vincent, K. A.; Armstrong, F. A.; Lenz, O. *J. Biol. Chem.* **2009**, *284*, 465–477.

(6) Cracknell, J. A.; Wait, A. F.; Lenz, O.; Friedrich, B.; Armstrong, F. A. *Proc. Natl. Acad. Sci. U.S.A.* **2009**, *106*, 20681–20686.

(7) Saggu, M.; Zebger, I.; Ludwig, M.; Lenz, O.; Friedrich, B.; Hildebrandt, P.; Lendzian, F. *J. Biol. Chem.* **2009**, *284*, 16264–16276.

(8) Goris, T.; Wait, A. F.; Saggu, M.; Fritsch, J.; Heidary, N.; Stein, M.; Zebger, I.; Lendzian, F.; Armstrong, F. A.; Friedrich, B.; Lenz, O. *Nat. Chem. Biol.* **2011**, *7*, 310–318.

(9) Bernhard, M.; Benelli, B.; Hochkoeppler, A.; Zannoni, D.; Friedrich, B. *Eur. J. Biochem.* **1997**, *248*, 179–186.

(10) Lenz, O.; Ludwig, M.; Schubert, T.; Burstel, I.; Ganskow, S.; Goris, T.; Schwarze, A.; Friedrich, B. *ChemPhysChem* **2010**, *11*, 1107–1119.

(11) Schink, B.; Schlegel, H. G. *Biochim. Biophys. Acta* **1979**, *567*, 315–324.

(12) Knuttel, K.; Schneider, K.; Erkens, A.; Plass, W.; Muller, A.; Bill, E.; Trautwein, A. X. *Bull. Pol. Acad. Sci., Chem.* **1994**, *42*, 495–511.

(13) Saggu, M.; Teutloff, C.; Ludwig, M.; Brecht, M.; Pandelia, M. E.; Lenz, O.; Friedrich, B.; Lubitz, W.; Hildebrandt, P.; Lendzian, F.; Bittl, R. *Phys. Chem. Chem. Phys.* **2010**, *12*, 2139–2148.

(14) Schneider, K.; Patil, D. S.; Cammack, R. *Biochim. Biophys. Acta* **1983**, *748*, 353–361.

(15) Saggu, M.; Ludwig, M.; Friedrich, B.; Hildebrandt, P.; Bittl, R.; Lendzian, F.; Lenz, O.; Zebger, I. *ChemPhysChem* **2010**, *11*, 1215–1224.

(16) Murgida, D. H.; Hildebrandt, P. *J. Phys. Chem. B* **2001**, *105*, 1578–1586.

(17) Feng, J. J.; Murgida, D. H.; Kuhlmann, U.; Utesch, T.; Mroginski, M. A.; Hildebrandt, P.; Weidinger, I. M. *J. Phys. Chem. B* **2008**, *112*, 15202–15211.

(18) Sezer, M.; Spricigo, R.; Utesch, T.; Millo, D.; Leimkuehler, S.; Mroginski, M. A.; Wollenberger, U.; Hildebrandt, P.; Weidinger, I. M. *Phys. Chem. Chem. Phys.* **2010**, *12*, 7894–7903.

(19) Wisitruangsakul, N.; Lenz, O.; Ludwig, M.; Friedrich, B.; Lendzian, F.; Hildebrandt, P.; Zebger, I. *Angew. Chem., Int. Ed.* **2009**, *48*, 611–613.

(20) Millo, D.; Pandelia, M. E.; Utesch, T.; Wisitruangsakul, N.; Mroginski, M. A.; Lubitz, W.; Hildebrandt, P.; Zebger, I. *J. Phys. Chem. B* **2009**, *113*, 15344–15351.

(21) Millo, D.; Pandelia, M. E.; Lubitz, W.; Hildebrandt, P.; Zebger, I. *Angew. Chem., Int. Ed. Engl.* **2011**, *50*, 2632–2634.

(22) Frielingdorf et al. Unpublished.

(23) Wackerbarth, H.; Klar, U.; Gunther, W.; Hildebrandt, P. *Appl. Spectrosc.* **1999**, *53*, 283–291.

(24) Moss, D.; Nabedryk, E.; Breton, J.; Mantele, W. *Eur. J. Biochem.* **1990**, *187*, 565–572.

(25) Arnold, K.; Bordoli, L.; Kopp, J.; Schwede, T. *Bioinformatics* **2006**, *22*, 195–201.

(26) Jormakka, M.; Tornroth, S.; Byrne, B.; Iwata, S. *Science* **2002**, *295*, 1863–1868.

(27) Humphrey, W.; Dalke, A.; Schulten, K. *J. Mol. Graphics* **1996**, *14*, 33–38.

(28) MacKerell; et al. *J. Phys. Chem. B* **1998**, *102*, 3586–3616.

(29) Baker, N. A.; Sept, D.; Joseph, S.; Holst, M. J.; McCammon, J. A. *Proc. Natl. Acad. Sci. U.S.A.* **2001**, *98*, 10037–10041.

(30) Dolinsky, T. J.; Nielsen, J. E.; McCammon, J. A.; Baker, N. A. *Nucleic Acids Res.* **2004**, *32*, W665–W667.

(31) Berks, B. C.; Page, M. D.; Richardson, D. J.; Reilly, A.; Cavill, A.; Outen, F.; Ferguson, S. J. *Mol. Microbiol.* **1995**, *15*, 319–331.

(32) Page, C. C.; Moser, C. C.; Chen, X. X.; Dutton, P. L. *Nature* **1999**, *402*, 47–52.

(33) Wackerbarth, H.; Hildebrandt, P. *ChemPhysChem.* **2003**, *4*, 714–724.

(34) Vincent, K. A.; Parkin, A.; Armstrong, F. A. *Chem. Rev.* **2007**, *107*, 4366–4413.

(35) To avoid confusion: only the reductive activation rate of the Ni_r-B state in ref 20 is taken into account for comparison.

(36) Léger, C.; Jones, A. K.; Roseboom, W.; Albracht, S. P. J.; Armstrong, F. A. *Biochemistry* **2002**, *41*, 15736–15746.

(37) Millo, D.; Bonifacio, A.; Ranieri, A.; Borsari, M.; Gooijer, C.; van der Zwan, G. *Langmuir* **2007**, *23*, 9898–9904.

(38) Fourmond, V.; Infossi, P.; Giudici-Orticoni, M. T.; Bertrand, P.; Léger, C. *J. Am. Chem. Soc.* **2010**, *132*, 4848–4857.

(39) Vincent, K. A.; Parkin, A.; Lenz, O.; Albracht, S. P. J.; Fontecilla-Camps, J. C.; Cammack, R.; Friedrich, B.; Armstrong, F. A. *J. Am. Chem. Soc.* **2005**, *127*, 18179–18189.

(40) Weidinger, I. M.; Murgida, D. H.; Dong, W. F.; Mohwald, H.; Hildebrandt, P. *J. Phys. Chem. B* **2006**, *110*, 522–529.

(41) Petrovic, J.; Clark, R. A.; Yue, H. J.; Waldeck, D. H.; Bowden, E. F. *Langmuir* **2005**, *21*, 6308–6316.

(42) Gross, R.; Pisa, R.; Sanger, M.; Lancaster, C. R. D.; Simon, J. *J. Biol. Chem.* **2004**, *279*, 274–281.